International Conference on Case Histories in Geotechnical Engineering

(2008) - Sixth International Conference on Case Histories in Geotechnical Engineering

14 Aug 2008, 2:15pm - 4:00pm

Settlement Analysis of Chek Lap Kok Trial Embankments with Probabilistic Extensions

Bak Kong Low
Nanyang Technological University (NTU), Singapore

Follow this and additional works at: https://scholarsmine.mst.edu/icchge

Part of the Geotechnical Engineering Commons

SETTLEMENT ANALYSIS OF CHEK LAP KOK TRIAL EMBANKMENTS WITH PROBABILISTIC EXTENSIONS

Bak Kong Low
School of Civil and Environmental Engineering
Nanyang Technological University (NTU)
Singapore 639798

ABSTRACT

Several test reclamation fills were constructed in Hong Kong in the 1980s on marine clay installed with prefabricated vertical drains prior to the construction of the Chek Lap Kok airport. Instrumentation data including settlement with time were available in the literature. The first part of this paper presents the author's deterministic settlement analysis for comparisons with the instrumented settlement-versus-time records of the marine clay. The second part of the paper illustrates, in the context of the Chek Lap Kok test fills, a new and efficient spreadsheet-based first-order reliability algorithm. Comparisons are made with results from Monte Carlo simulations. The proposed reliability method can be applied to other stand-alone deterministic numerical packages via the established response surface method.

INTRODUCTION

The Chek Lap Kok test reclamation fill on marine clay (in the 1980s) was part of a larger reclamation project for the construction of a Hong Kong replacement airport (which started operation in 1997). The objective of the test fill was to investigate the feasibility of reclamation over soft marine clay and the effectiveness of vertical drains in accelerating consolidation. The main test area, located about 200 m offshore and 100 m square in plan, was divided into quadrants: one was a control area, with no treatment of the marine clay, the remaining three quadrants were installed with vertical drains at different spacing through about 7-m thick marine clay. The offshore geotechnical investigations, the test fill, and the instrumentation program were described in substantial detail by Foott et al. (1987) and Koutsoftas et al. (1987), and further studied in Choa et al. (1990).

In this paper a deterministic numerical method (Low, 2003) written in the VBA programming environment of Microsoft Excel spreadsheet is first described for consolidation analysis involving vertical drains. The program accounts—in an approximate manner—for stage loading, load reduction due to fill submergence, delayed vertical drain installation, changes in length of vertical drainage path with time, and variation of soil stress history with depth. Comparisons are then made between the results of program analysis and the instrumented settlement records of the soft clay beneath the Chek Lap Kok test fills. The paper then extends the analysis probabilistically, by applying the new efficient and intuitive first-order reliability algorithm of Low and Tang (2007).

DETERMINISTIC CONSOLIDATION ANALYSIS INVOLVING VERTICAL DRAINS

The program for deterministic analysis uses Barron's solution for equal vertical strain of consolidation due to radial drainage and Carillo's equation for combined radial and vertical drainage. A practical algorithm for prediction of rate of settlement was adopted because, even in the relatively simple approach adopted here, 15 or more values of individual input parameters were required. The uncertainties associated with some of these parameters will limit the accuracy of prediction even if sophisticated models are used. The computational algorithm in the program is not fully rigorous, because idealizations and approximations have been made. Nevertheless, limited comparisons made by the author suggest that the degree of accuracy achieved is adequate for the purpose in hand. Its relative simplicity also gave rise to some insights on parametric relationships and sensitivities.

Figure 1 shows example input data for analysis using the program. Any system of units can be used, provided consistency is observed. This means that if length (e.g. thickness, elevation, drain spacing, drain diameter) is in meter and time in day, then the units for the coefficients of consolidation c_v and c_h have to be in m^2/day.

In Fig. 1 the units are meter, m^2/day, day, kN/m^3, kN/m^2, as appropriate. The program code of the function *VDrainSt* in row 25 is shown in Fig. 2.17 of Low (2003). The function need only be entered in the first cell (cell A25), followed by autofilling to the right. The first 15 parameters in the top half
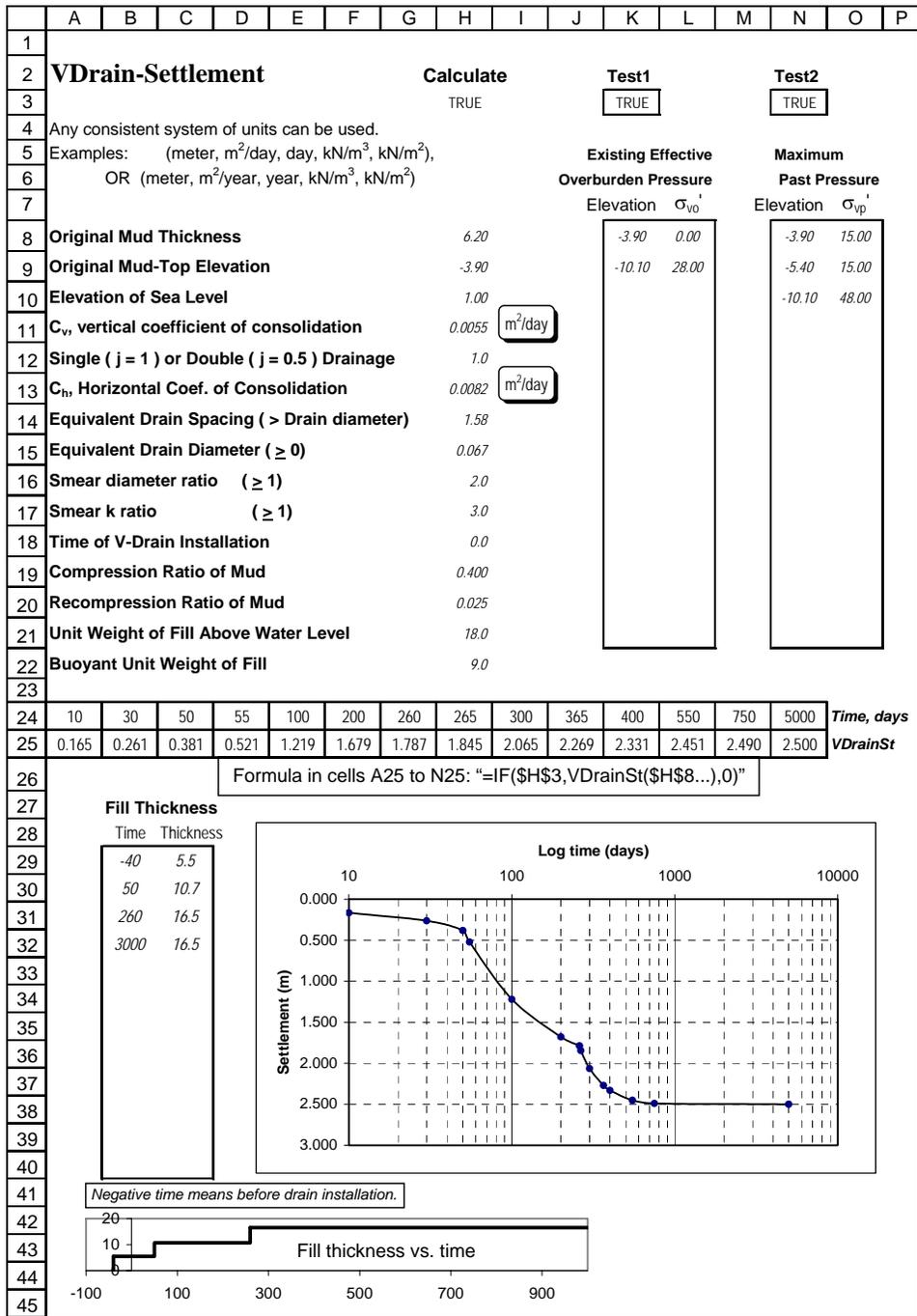
Fig. 1. Approximate analysis of consolidation settlement using user-created VBA function in Microsoft Excel spreadsheet.

of Fig. 1 are self-explanatory. The next three sets of data in Fig. 1 define staged loading (increase in fill thickness with time), initial effective vertical stress profile, and maximum past pressure profile, as explained in Low (2003).

Example Program Input and Output

In Fig. 1, the vertical drain is installed at time 0. The time in row 24 means number of days since the installation of the vertical drains. Had time zero been used to specify the time of the first increment of the fill thickness in Fig. 1, the time of the vertical drain installation would be 40 days (cell H18); the time values in row 24 would then denote the number of days since the time of the first increment of the fill thickness.

The time values in row 24 are input by user. The settlement versus time curve will exhibit kinks at time values corresponding to increase in fill thickness. Hence, it is desirable to specify these time values (50 and 260 days for the

case in Fig. 1) and shortly after (e.g., 55 and 265 days). The other time values can be arbitrarily spaced, or spaced at regular intervals, the guideline being to obtain a relatively smooth curve of settlement versus time plot.

The c_v and c_h values of 0.0055 and 0.0082 m^2/day in Fig. 1 correspond to about 2.0 m^2/year and 3.0 m^2/year, respectively. The same template of Fig. 1 can be used to obtain the rate of settlement for the case with no vertical drains. This is done by setting the value of c_h to zero; the other vertical-drain related parameters (cells H14:H17) can be left at their typical values and will have no effect on computed results when c_h is set to zero. Figure 2 compares the rate of settlement with and without vertical drains. Except for the value of c_h, all other parameters are as shown in Fig. 1.
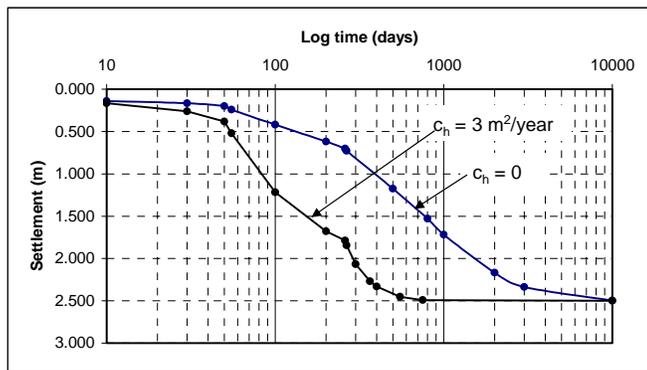

Fig. 2. Comparing theoretical settlement rates with and without vertical drains, for the case of Fig. 1.

If the project is on land and has no submergence effect (e.g. a highway embankment constructed on soft clay), it is only necessary to input the buoyant unit weight of fill as equal to the unit weight of fill above water level.

Computational Rationale in the Program and Limitations

The program *VDrainSt* combines vertical and horizontal drainage using Carillo's equation. The depth-dependent degree of consolidation due to vertical flow and the equal-strain solution of the degree of consolidation due to radial flow are used. The thickness of fill versus time is part of the input. For each incremental thickness, the degrees of consolidation for vertical and radial drainage are combined to obtain the average degree of consolidation at the particular depth z. One value of the average degree of consolidation U_{vh} will be computed for each fill thickness increment that has already taken place. Each value of U_{vh} is multiplied by the incremental fill load (equal to incremental fill thickness × fill unit weight) to obtain the increase in effective vertical stress in the clay due to the particular fill increment. The total increase in effective vertical stress (up to the time in question) due to all the fill increments which have taken place is obtained by superposition. To account for the variation of the stress history (initial effective vertical stress and maximum past pressure) of the marine clay with depth, the program divides the marine clay into 21 sub-

layers of equal thickness. For each sub-layer the initial effective vertical stress and the maximum past pressure are interpolated by the program from the soil stress history profile provided by the user. The number of points defining variation of initial effective vertical stress and maximum past pressure with depth can be as many as justified by the certainty of knowledge concerning them. The induced consolidation settlement will differ from one sub-layer to another if the initial effective vertical stress and the maximum past pressure vary with depth, which is typical. The program obtains the consolidation settlement up to the time in question by summing the compression of all the sub-layers.

The program is meant for analysis where the values of the coefficients of consolidation (in the vertical and radial directions) and the compression ratios are assumed to be independent of the magnitude of the stress increment. Unloading is not considered. Also, the coefficients of consolidation in the recompression range are assumed to be the same as those in the virgin compression range. For the soft marine clay in the Chek Lap Kok project where the difference between maximum past pressure and initial effective vertical stress is small compared with the magnitude of the applied stress, little error is introduced by the assumption. For other situations, the likely higher values of the coefficients of consolidation in recompression than in virgin compression may need to be explicitly accounted for if the prediction of settlement rate is to be realistic.

ANALYSIS OF CHEK LAP KOK TEST EMBANKMENTS

The program-computed results will be compared with the measured settlement record of the marine clay.

The following values of coefficients of consolidation are used in program computations:

Undisturbed c_v = 1 m^2/year	(Choa et al., 1990)
Undisturbed c_h = 3.7 m^2/year	(Koutsoftas et al., 1987)
Remolded c_h = 0.8 m^2/year	(Choa et al., 1990)

The original c_v and c_h values of 1 m^2/year and 3.7 m^2/year are divided by 365 days to obtain 0.00274 m^2/day and 0.0101 m^2/day, respectively. The effect of smear is accounted for using smear diameter ratio s = 2 and smear permeability ratio (k_h/k_s) = 3.7/0.8 = 4.63 as part of the input.

Basis for the Values of Other Parameters Used in the Program Computations

Based on Choa et al. (1990)'s studies of the available soft clay data, a compression ratio C_R of 0.36 will be used. The recompression ratio C_{RR} is about 5%-10% of the compression ratio. For analysis 7% is assumed. Note that for the soft marine clay layer the recompression settlement is negligible when compared to the settlement due to virgin compression.

As mentioned earlier, a c_v value of 1 m²/year is used in computation. Although there is evidence that in the recompression range c_v could be much higher, the assumption of the same value of c_v for virgin compression as well as for recompression will introduce little error because recompression settlement is negligible, and also the difference between initial effective vertical stress and maximum past pressure is small compared with the applied stress.

Another factor to be resolved is the length of the drainage path in the vertical direction. For double drainage condition (top and bottom surface of soft clay open), it is equal to half the layer thickness, corresponding to $j = 0.5$ in the program. For single drainage condition (top surface open but bottom surface closed), it is equal to the entire soft clay thickness, or $j = 1$ in the program. For purpose of comparison, both conditions will be analyzed. It will be seen that in the presence of simultaneous radial drainage to the vertical drains, the rate of consolidation settlement is not very sensitive to the values of the length of drainage path in the vertical direction or of the coefficient of consolidation (c_v) in the vertical direction.

The above paragraphs have provided the basis for the values of the main input parameters for analysis using the program. Other necessary information such as thickness of the soft marine clay and variation of fill thickness with time are based on the Hong Kong Geotechnical Control Office's GCO.4/90 Drawings #1-10, made available to Choa et al. in their 1990 studies. The soil stress profile (initial effective stress and maximum past pressure) is based on Choa et al. (1990)'s studies of available data. The measured range of settlement for each test embankment quadrant is based on GCO.4/90 Drawing #1.

Comparing Program Computations with Measured Settlements

Results from analyses using the program are plotted in Figs. 3 and 4, corresponding to the 1.5 m band-drain-spacing quadrant and the 3 m band-drain-spacing quadrant, respectively. The lists of input values for each quadrant are also shown in the respective figures. For comparison, the measured range of settlements is also plotted. Note that there are two computed curves for each quadrant: the upper (slower) curve (with "o" markers) represents single drainage condition ($j = 1$), while the lower (faster) curve (with "∗" markers) represents double drainage condition ($j = 0.5$).

The following may be observed in Fig. 3:

1. Whether single drainage or double drainage is assumed has negligible influence on the computed rate of settlement. This is because for 1.5 m band-drain-spacing, consolidation due to radial drainage far outweighs that due to vertical drainage.
2. The shape of the computed curves is similar to the shape of the measured range, both reflecting the staged loading. The computed rate of settlement is only slightly slower than the measured rate.

3. The computed final consolidation settlement (≈ 2.7 m) is slightly smaller than the average of the measured range of settlement, by about 0.2 m.

Similar observations may be made for Fig. 4, except that the difference between single drainage condition and double drainage condition is somewhat larger than in Fig. 3. This is due to the increasing role of drainage in the vertical direction in this quadrant where the band-drains are spaced further apart (3 m) than in Fig. 3.

The discrepancies in the computed and measured *magnitude* of final settlement for the band-drain quadrants may be attributed to undrained settlement and secondary compression settlement, both of which are not accounted for in the program, and to uncertainties (probably small) associated with the instrumented results. As for the *rate* of settlement, comparison of the computed and measured curves seem to support double drainage conditions (i.e. $j = 0.5$) for the control quadrant and the 3 m band-drain-spacing quadrant. The computations also indicate the importance of taking the smear effect into account.

In both Figs. 3 and 4, the discrepancies between the computed curves and the measured ranges are partly attributable to the underestimation of final consolidation settlement by the program. The final consolidation settlements are functions of C_R, C_{RR}, stress history, and applied loadings, but are not affected by the values of the rate parameters c_v and c_h, nor by the idealizations and approximations in the modeling of excess pore pressure dissipation in the program.

The program-computed results will be even closer to the observed settlement curves if different values of c_h and compression ratios are used, but such speculations belong to the realm of back-analysis and hindsight and will not be pursued here. Instead, something will be said about sensitivity.

SENSITIVITY CONSIDERATIONS

The accuracy of design and prediction is often limited not so much by the lack of rigorousness in the analytical model as by the uncertainties associated with the input parameters used in the analysis. This is particularly so when the number of parameters is large, each with its own degree of uncertainty. In these circumstances parametric and sensitivity studies are useful, to identify situations in which uncertainty in a parameter will have significant influence in the calculated results and situations in which the uncertainty is of little consequence. For instance, whether to use lab c_v or field c_v and what vertical drainage length to assume are certainly much more important questions for the control quadrant (without vertical drains) than for the 1.5 m band drain quadrant. Whenever possible, one should incorporate the uncertainty of the various parameters into the computational procedure, so that relationships/charts/equations can be developed to give the likely range of the settlement rate, in addition to the rate based on mean parametric values.
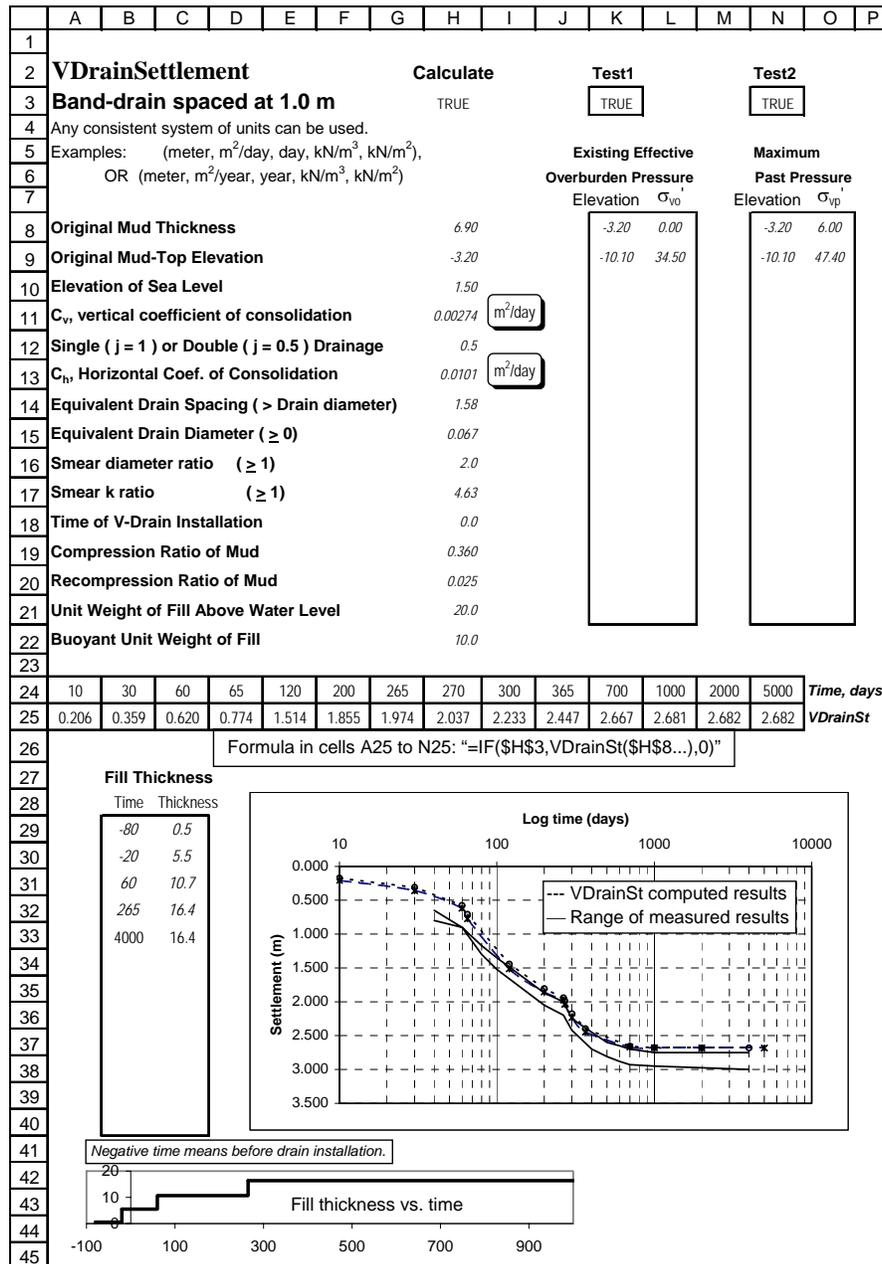
The spreadsheet figure contains the following data:

VDrainSettlement
Band-drain spaced at 1.0 m

		Calculate	Test1	Test2
		TRUE	TRUE	TRUE

Any consistent system of units can be used.
Examples: (meter, m²/day, day, kN/m³, kN/m²),
OR (meter, m²/year, year, kN/m³, kN/m²)

			Existing Effective Overburden Pressure		Maximum Past Pressure	
			Elevation	σ_{vo}'	Elevation	σ_{vp}'
Original Mud Thickness	6.90		-3.20	0.00	-3.20	6.00
Original Mud-Top Elevation	-3.20		-10.10	34.50	-10.10	47.40
Elevation of Sea Level	1.50					
C_v, vertical coefficient of consolidation	0.00274	m²/day				
Single (j = 1) or Double (j = 0.5) Drainage	0.5					
C_h, Horizontal Coef. of Consolidation	0.0101	m²/day				
Equivalent Drain Spacing (> Drain diameter)	1.58					
Equivalent Drain Diameter (≥ 0)	0.067					
Smear diameter ratio (≥ 1)	2.0					
Smear k ratio (≥ 1)	4.63					
Time of V-Drain Installation	0.0					
Compression Ratio of Mud	0.360					
Recompression Ratio of Mud	0.025					
Unit Weight of Fill Above Water Level	20.0					
Buoyant Unit Weight of Fill	10.0					

10	30	60	65	120	200	265	270	300	365	700	1000	2000	5000	Time, days
0.206	0.359	0.620	0.774	1.514	1.855	1.974	2.037	2.233	2.447	2.667	2.681	2.682	2.682	VDrainSt

Formula in cells A25 to N25: "=IF($H$3,VDrainSt($H$8...),0)"

Fill Thickness

Time	Thickness
-80	0.5
-20	5.5
60	10.7
265	16.4
4000	16.4

Negative time means before drain installation.

Fill thickness vs. time

Fig. 3. Program-computed results for Chek Lap Kok 1.5 m band-drain-spacing test fill quadrant, and comparison with measured settlement range. The c_v and c_h values of 0.00274 and 0.0101 m²/day correspond to 1 m²/yr and 3.7 m²/yr respectively.

Figure 3 shows that the rate of settlement is not sensitive to whether drainage occurs at both the top and bottom boundaries of the marine clay (i.e. $j = 0.5$), or at the top boundary only (i.e. $j = 1$), for the two sets of points are practically the same, reflecting the predominant role of radial drainage in the quadrant with band drains spaced at 1.5 m in triangular grids. The sensitivity of the settlement rate to c_v can also be inferred from the same figure. One notes that the time factor for vertical flow depends on $c_v/(j \times$ clay thickness$)^2$; therefore if the values of c_v and j change such that the ratio c_v/j^2 remains the same, the settlement rate will not change. This means the results for ($j = 1$, $c_v = 4$ m²/year) will be identical to the ($j = 0.5$, $c_v = 1$ m²/year) curve (marked "∗") in Fig. 3; but the latter is very close to the ($j = 1$, $c_v = 1$ m²/year) points (marked "o"). It follows that ($j = 1$, $c_v = 4$ m²/year) ≈ ($j = 1$, $c_v = 1$ m²/year). Hence computed settlement curve is not sensitive to the uncertainty associated with the value of c_v in this quadrant, where the soft marine clay is about 7 m thick and the band drains are spaced at 1.5 m on triangular grids.

Similarly, if the values of c_h, equivalent drain spacing d_e, and drain diameter d_w all change but in such a way that the ratio $c_h/(d_e^2.F_s(n))$ remains constant, then the computed settlement versus time curves will be the same. These anticipations can be verified using the program.

	A	B	C	D	E	F	G	H	I	J	K	L	M	N	O	P
2	**VDrainSettlement**							**Calculate**			**Test1**			**Test2**		
3	**Band-drain spaced at 3.0 m**							TRUE			TRUE			TRUE		
4	Any consistent system of units can be used.															
5	Examples: (meter, m²/day, day, kN/m³, kN/m²),										**Existing Effective**			**Maximum**		
6	OR (meter, m²/year, year, kN/m³, kN/m²)										**Overburden Pressure**			**Past Pressure**		
7											Elevation σ_{vo}'			Elevation σ_{vp}'		
8	**Original Mud Thickness**							6.60			-3.20 0.00			-3.20 6.00		
9	**Original Mud-Top Elevation**							-3.20			-9.80 33.00			-9.80 45.60		
10	**Elevation of Sea Level**							1.50								
11	**C_v, vertical coefficient of consolidation**							0.00274	m²/day							
12	**Single (j = 1) or Double (j = 0.5) Drainage**							0.5								
13	**C_h, Horizontal Coef. of Consolidation**							0.0101	m²/day							
14	**Equivalent Drain Spacing (> Drain diameter)**							3.15								
15	**Equivalent Drain Diameter ($\geq$ 0)**							0.067								
16	**Smear diameter ratio ($\geq$ 1)**							2.0								
17	**Smear k ratio ($\geq$ 1)**							4.63								
18	**Time of V-Drain Installation**							0.0								
19	**Compression Ratio of Mud**							0.360								
20	**Recompression Ratio of Mud**							0.025								
21	**Unit Weight of Fill Above Water Level**							20.0								
22	**Buoyant Unit Weight of Fill**							10.0								
24	10	25	26	55	56	80	100	200	265	270	365	800	1500	5000	*Time, days*	
25	0.184	0.229	0.235	0.399	0.407	0.637	0.803	1.290	1.465	1.502	1.828	2.290	2.418	2.441	*VDrainSt*	
26	Formula in cells A25 to N25: "=IF($H$3,VDrainSt($H$8...),0)"															

Fill Thickness

Time	Thickness
-80	0.5
-20	5.5
25	7.8
55	10.7
265	14.4
3000	14.4

Negative time means before drain installation.
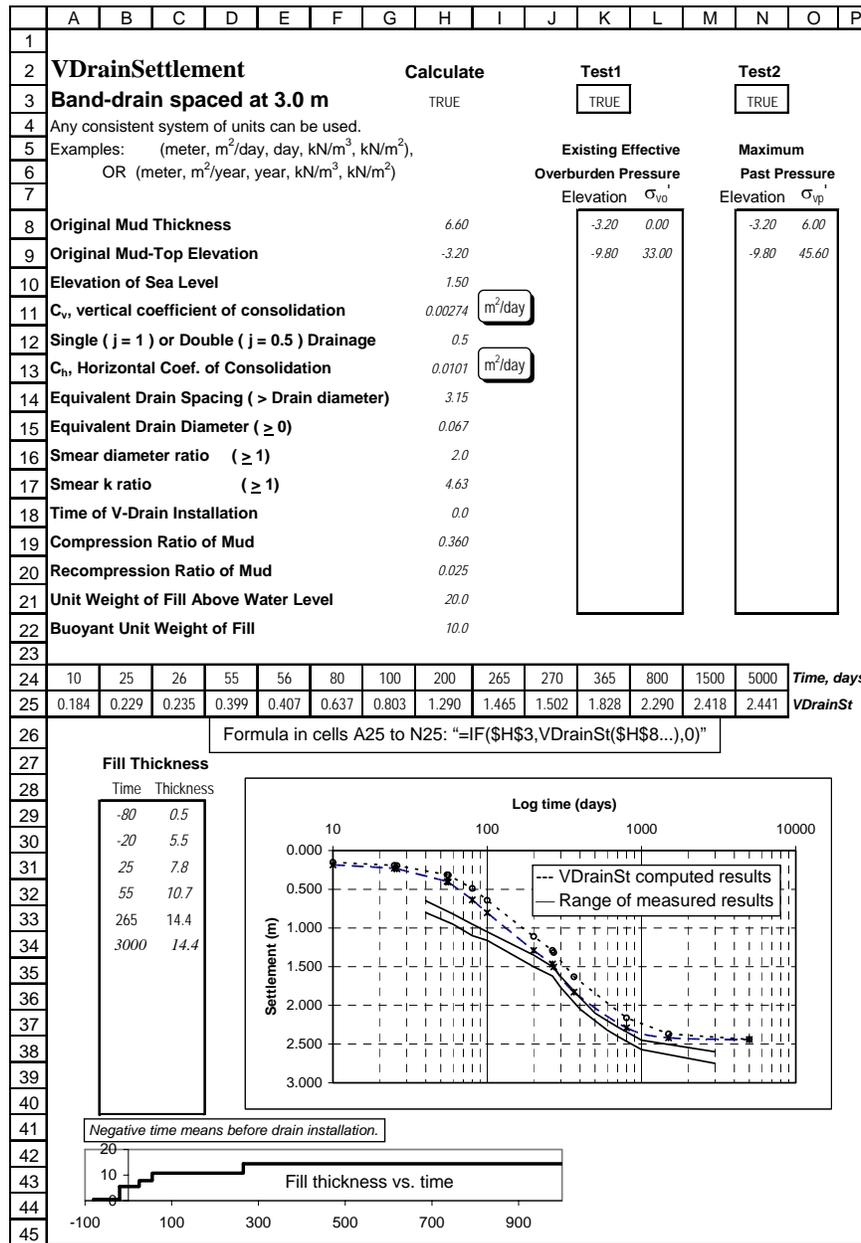
Fill thickness vs. time

Fig. 4. Program-computed results for Chek Lap Kok 3.0 m band-drain-spacing test fill quadrant, and comparison with measured settlement range. The c_v and c_h values of 0.00274 and 0.0101 m²/day correspond to 1 m²/yr and 3.7 m²/yr respectively.

The computed settlement rate for the 3 m band-drain-spacing quadrant, Fig. 4, is by comparison more sensitive to variations in the ratio c_v/j^2. This is readily comprehensible because the $c_h/(d_e^2.F_s(n))$ value for this quadrant is only 22% of the $c_h/(d_e^2.F_s(n))$ value for the 1.5 m band-drain-spacing quadrant; the role of radial drainage is correspondingly less dominant in the 3-m band-drain-spacing quadrant. (Both quadrants have about the same thickness of marine clay).

It follows that the sensitivities of the parameters which affect the rate of settlement (c_v, c_h, length of vertical drainage path H, equivalent drain spacing d_e, and drain diameter d_w) can be studied via two terms: c_v/H^2, and $c_h/[d_e^2.F_s(n)]$, where $n = d_e/d_w$.

Assuming that the time for consolidation is the same for both vertical flow and horizontal flow (i.e., no time lag between the start of vertical flow and the start of radial flow), Low (2003) obtained the following chart (Fig. 5) which displays the sensitivity of the average degree of consolidation for combined radial and vertical drainage (U_{vh}) to the λ values and hence to the $c_h H^2 / c_v d_e^2 F(n)$ ratio. The chart is therefore convenient for assessing how deviations from the assumed values of the parameters will affect the calculated average

degree of consolidation for simultaneous vertical and radial consolidation. Note that the uppermost curve, with $\lambda = 0$, is the case with no vertical drains.
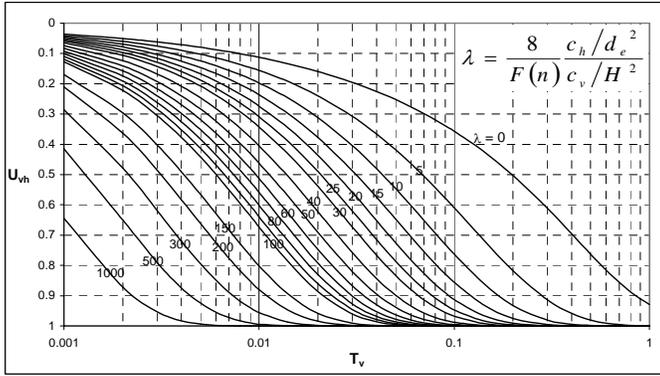

$$\lambda = \frac{8}{F(n)} \frac{c_h / d_e^2}{c_v / H^2}$$

Fig. 5. Average degree of consolidation for combined radial and vertical drainage (U_{vh}) as a function of the lumped parameter λ.

Yet another alternative is to perform reliability analysis and reliability-based design accounting explicitly for the estimated uncertainties of the parameters. The classical method of computing the Hasofer-Lind reliability index is intricate when correlation, autocorrelation, and nonnormal distributions are involved and when the performance function is complicated or implicit. These hitherto tedious problems can be solved, with relative ease and transparency, using spreadsheet-automated constrained optimization and the expanding ellipsoid perspective (Low and Tang, 2004, 2007). By this perspective, the quadratic form defining the Hasofer-Lind index is visualized as a tilted multi-dimensional ellipsoid (centred at the mean μ or equivalent mean μ^N) in the original space of the random variables; there is no need to diagonalize the covariance or correlation matrix. The concepts of coordinate transformation and frame-of-reference rotation are not required. Iterative searching and partial derivatives are automatic using constrained optimization in the ubiquitous spreadsheet platform. The versatility of the spreadsheet constrained optimization approach is enhanced when used in combination with user-defined functions coded in the programming environment of the spreadsheet, for example the Visual Basic (VBA) programming environment of the Microsoft Excel spreadsheet software. This means that the performance function can be implicit, iterative, and based on numerical methods (Low et al. 2007).

In the following section the Low and Tang (2007) new and efficient algorithm is used to perform reliability analysis.

RELIABILITY ANALYSIS

The Hasofer-Lind index for cases with correlated normal random variables and the first-order reliability method (FORM) for cases with correlated nonnormals are well explained in Ang and Tang (1984), Haldar and Mahadevan (1999), and Baecher and Christian (2003), for example. The potential inadequacies of FORM in some cases have been

recognized, and more refined alternatives proposed, for example in Der Kiureghian et al. (1987). On the other hand, the usefulness and accuracy of FORM in most applications are well recognized, for instance in Rackwitz (2001). The focus in the sections below is on FORM, which includes the Hasofer-Lind index as a special case. The case in Fig. 3 will be analyzed probabilistically using the Low and Tang (2007) new algorithm for the FORM, which obtains the same solution as the widely known classical FORM procedure, but more intuitively and directly, and on a ubiquitous platform. Figure 6 shows the difference between the 2007 method (used herein) and the 2004 method.

Minimize β by varying x_i (Low and Tang, 2004)

$$\beta = \min_{\underline{x} \in F} \sqrt{\left[\frac{x_i - \mu_i^N}{\sigma_i^N} \right]^T [\underline{R}]^{-1} \left[\frac{x_i - \mu_i^N}{\sigma_i^N} \right]}$$

by changing x_i (via Excel's *Solver*), and subject to $g(\underline{x}) = 0$.

For each trial x_i, the Rackwitz-Fiessler equivalent normal transformation is peformed:

$$\sigma^N = \frac{\phi\{\Phi^{-1}[F(x)]\}}{f(x)} ; \qquad \mu^N = x - \sigma^N \times \Phi^{-1}[F(x)]$$

Minimize β by varying n_i (Low and Tang, 2007)

$$\beta = \min_{\underline{x} \in F} \sqrt{[n]^T [\underline{R}]^{-1} [n]}$$

by changing n_i (via Excel's *Solver*), and subject to $g(\underline{x}) = 0$.

For each trial n_i, the value of the original basic random variable x_i is computed automatically:

$$x_i = F^{-1}[\Phi(n_i)]$$

The above inverse distribution functions are either closed forms, or computed via a refined Newton method.

Fig. 6. Two methods compared: 2004 method requires computation of equivalent normal means and equivalent normal standard deviations; the 2007 alternative method does not.

Limit State Surface (LSS) and Performance Function g(x)

The following three aspects are studied:
(i) the magnitude of the ultimate consolidation settlement s_{cf};
(ii) the degree of consolidation U at time = 1 year;
(iii) the consolidation settlement remaining (s_r) at time = 1 year, where $s_r = s_{cf} - s_{1\,yr}$.

The performance functions (also called limit state functions) are, respectively:

$$g_1(\underline{x}) = Limiting\ s_{cf} - s_{cf} \qquad (1)$$

$$g_2(\underline{x}) = U\text{ - }\textit{Limiting U} \qquad (2)$$

$$g_3(\underline{x}) = \textit{Limiting }s_r - s_r \qquad (3)$$

in which s_{cf}, U, and s_r are functions of the various inputs ($\underline{x}$) shown in Fig. 3, including parameters of compressibility, consolidation rate, staged loading, and stress history.

The term "limiting" connotes "acceptable" or "permissible". Positive $g(\underline{x})$ values correspond to safe domain, and negative $g(\underline{x})$ values correspond to unsafe domain. Hence, for $g_1(\underline{x})$ and $g_3(\underline{x})$, by virtue of 'smaller settlement is safer', safe domain is indicated when *Limiting $s_{cf} > s_{cf}$*, and *Limiting $s_r > s_r$*. In contrast, for $g_2(\underline{x})$, by virtue of 'larger degree of consolidation is safer', safe domain is indicated when *U > Limiting U*. These are illustrated schematically in the plane in Figs. 7 and 8. Also, for all three performance functions, the parametric surface that separates safe combinations of parameters from unsafe combinations of parameters is the *limit state surface (LSS),* given by $g(\underline{x}) = 0$.

Distinguishing Postive and Negative Reliability Indices

In Fig. 7, when the limiting (i.e. permissible) ultimate consolidation settlement is s_{L1}, the settlement evaluated at mean-value point (s_μ) is already in the unsafe zone ($>s_{L1}$). Under this circumstance the computed reliability index β must be regarded as negative: it is the minimum distance (in units of directional standard deviations) from the *unsafe m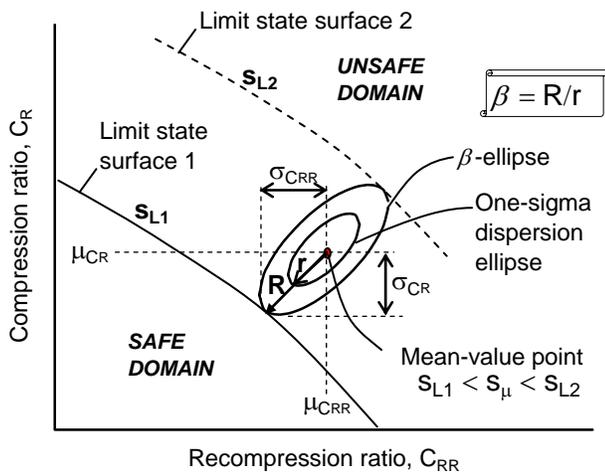ean-value point* to the *safe boundary* defined by LSS1. On the other hand, if a higher permissible settlement (s_{L2}) is specified, the mean-value point is in the safe zone, and the reliability index β is positive: it is the minimum distance (in units of directional standard deviations) from the *safe mean-value point* to the *unsafe boundary* defined by LSS2.

Fig. 7. Illustration of reliability index in the plane for performance function $g_1(\underline{x})$. With respect to LSS1, reliability index β is negative; with respect to LSS2, β is positive.

In contrast, in Fig. 8, the reliability index β with respect to LSS1 (for which limiting $U = U_{L1}$) is positive while that with respect to LSS2 (for which limiting $U = U_{L2}$) must be treated as negative.

Reliability Analysis for Different Limiting State Surfaces

The Low and Tang (2007) procedure for FORM can deal with various correlated nonnormal distributions (lognormal, general beta, gamma, type 1 extreme, exponential, …). In this study only correlated lognormals are illustrated. The values of C_R, C_{RR}, c_v and c_h in Fig. 3 are taken to be the mean values (Para1) in Fig. 9. Assumed values of standard deviations are used, for illustrative purpose. Positive correlations, logical between C_R and C_{RR} and between c_v and c_h, are modeled.

The originally deterministic set-up of Fig. 3 and the reliability method of Fig. 9 are coupled easily by replacing the C_R, C_{RR}, c_v and c_h values (cells H19, H20, H11 and H13) of Fig. 3 with the formulas "=Z28", "=Z29", "=Z30" and "Z31" which refer to the x* values in Fig. 9. The performance function $g_1(\underline{x})$ is, by Eq. (1), "=W34–N25", where cell W34 has value 2.0 for this analysis. The computed β index is 1.485, treated as (−1.485) because the mean-value point is in the unsafe zone as indicated by the negative $g(\underline{x})$ value when the n_i values were initialized to zeros. (Files illustrating the Low and Tang 2007 approach are available at http://alum.mit.edu/www/bklow.)

By varying the s_{limit} value (cell W34) between 1.2 and 4.8 at intervals of 0.2, and each time re-computing the β index, 19 values of β were obtained as shown in Fig. 10.

Obtaining Probability of Failure (P_f) and CDF from β Indices

Referring to Fig. 7, for $s_{L1} = 2.0$ m and $\beta = -1.485$ from Fig. 9, the probability of failure P_f is the integration of the probability density over the entire unsafe zone ($s > s_{L1}$). A good estimate
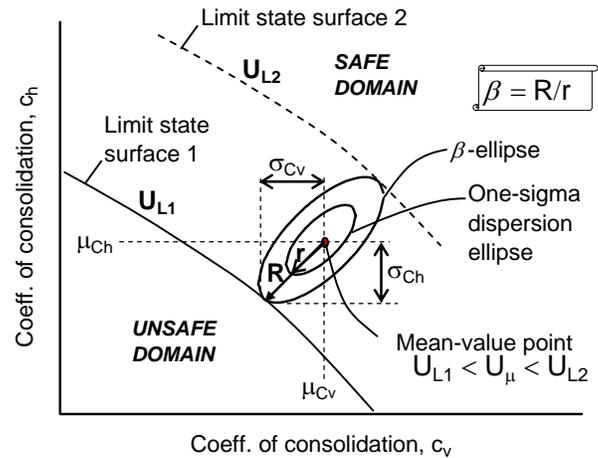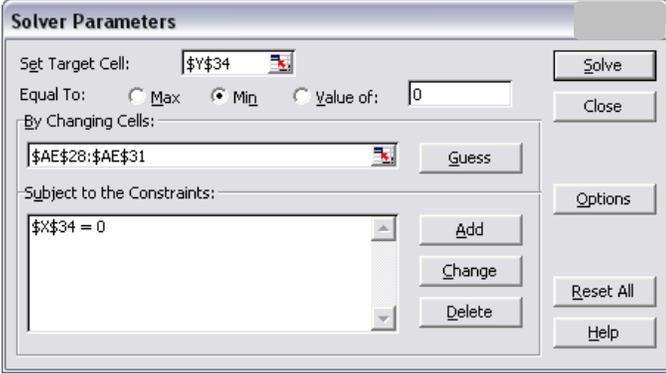

Fig. 8. Illustration of reliability index in the plane for performance function $g_2(\underline{x})$. With respect to LSS1, reliability index β is positive; with respect to LSS2, β is negative.

	V	W	X	Y	Z	AA	AB	AC	AD	AE
27			Para1	Para2	x_i^*	Correlation matrix				n_i
28	Lognormal	C_R	0.36	0.070	0.3534	1	0.7	0	0	0
29	Lognormal	C_{RR}	0.025	0.005	0.0245	0.7	1	0	0	0
30	Lognormal	c_v	0.00274	0.0005	0.0027	0	0	1	0.7	0
31	Lognormal	c_h	0.0101	0.0020	0.0099	0	0	0.7	1	0
32										
33		s_{limit}	$g(\underline{x})$	β						
34			2.0	-0.6346	0.000					

Solver Parameters

Set Target Cell: $Y$34

Equal To: ○ Max ● Min ○ Value of: 0

By Changing Cells:
$AE$28:$AE$31   [Guess]

Subject to the Constraints:
$X$34 = 0   [Add] [Change] [Delete]

[Solve] [Close] [Options] [Reset All] [Help]

	V	W	X	Y	Z	AA	AB	AC	AD	AE
27			Para1	Para2	x_i^*	Correlation matrix				n_i
28	Lognormal	C_R	0.36	0.070	0.2655	1	0.7	0	0	-1.485
29	Lognormal	C_{RR}	0.025	0.005	0.0199	0.7	1	0	0	-1.054
30	Lognormal	c_v	0.00274	0.0005	0.0027	0	0	1	0.7	-9E-08
31	Lognormal	c_h	0.0101	0.0020	0.0099	0	0	0.7	1	-9E-08
32										
33		s_{limit}	$g(\underline{x})$	β						
34			2.0	0.0000	1.485					

Fig. 9. Initially the n_i values were zeros, and $g(\underline{x})$ exhibits negative values. Hence, the computed β value must be treated as negative ($\beta = -1.485$).

of P_f can often be obtained by the following established relationship:

$$P_f \approx \Phi(-\beta) \qquad (4)$$

In Eq. (4), $\Phi(.)$ is the cumulative distribution of the standard normal variate. Probability of failure is often of interest for ultimate limit states. However, for serviceability limit states such as Eqs. (1), (2) and (3) for s_{cf}, U and s_r, it would be of interest to obtain the cumulative distribution (CDF) from the β indices, as follows:

$$g_1(\underline{x}) = Limiting\ s_{cf} - s_{cf} : \qquad CDF = \Phi(\beta) \qquad (5)$$

$$g_2(\underline{x}) = U - Limiting\ U : \qquad CDF = \Phi(-\beta) \qquad (6)$$

$$g_3(\underline{x}) = Limiting\ s_r - s_r : \qquad CDF = \Phi(\beta) \qquad (7)$$

The reason for Eqs. (5) and (7) being different from Eq. (6) is readily appreciated if one notes that, for Eq. (5) and (7), CDF
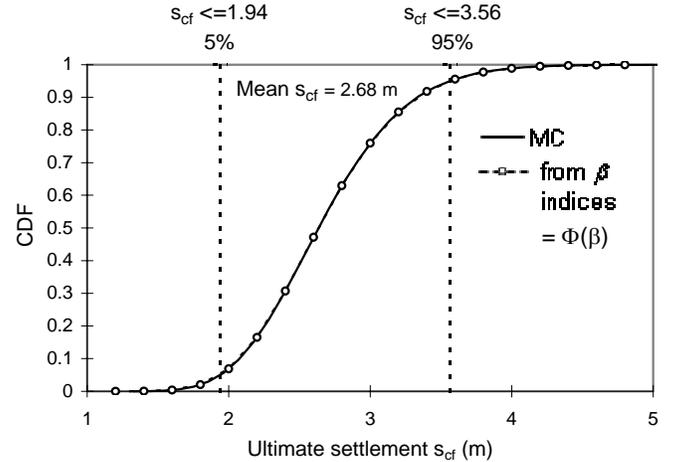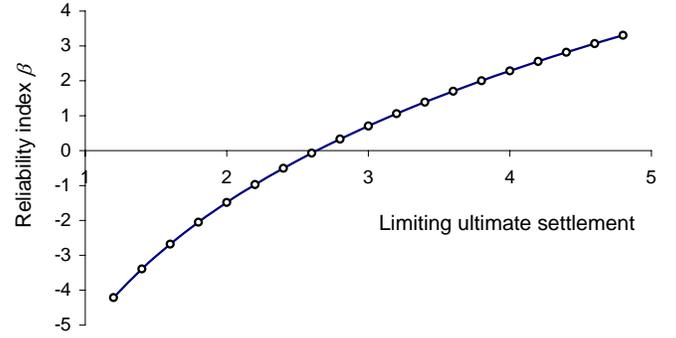

Fig. 10. Reliability indices for different limiting ultimate settlements, and comparison of CDF based on β indices with CDF from Monte Carlo simulations.

$= P[s < s_{limit}] = 1 - P[s > s_{limit}] = 1 - P_f$. In contrast, for Eq. (6), CDF $= P[U < U_{limit}] = P_f$.

As shown in Fig. 10, the CDF based on 19 values of β indices is practically indistinguishable from the CDF from 5000 realizations of Monte Carlo simulation using the software @RISK (http://www.palisade.com). For the assumed statistical input and correlation structure, the 90% confidence interval of the ultimate consolidation settlement is (1.94 m, 3.56 m). The measured ultimate settlement shown in Fig. 3 is within this interval. Other confidence intervals can also be read from Fig. 10. For example, a narrower 50% confidence interval (still bracketing the observed settlement) can be read off from the CDF values of 25% and 75%. Considerations such as this should be much more useful in the design stage than a deterministic analysis which yields a single ultimate settlement value with no indication at all of the effect of uncertainties (parametric, modeling, and others) on the predicted ultimate settlement.

Figures 11 and 12 show the CDF curves obtained from reliability indices (Eqs. (6) and (7)), for the degree of consolidation (U) and the consolidation settlement remaining (s_r), respectively, at time = 1 year. As in Fig. 10, the two CDF curves in Figs. 11 and 12, based on 17 and 23 values of β indices, respectively, are practically the same as the CDF curves from 5000 realizations of Monte Carlo simulation.
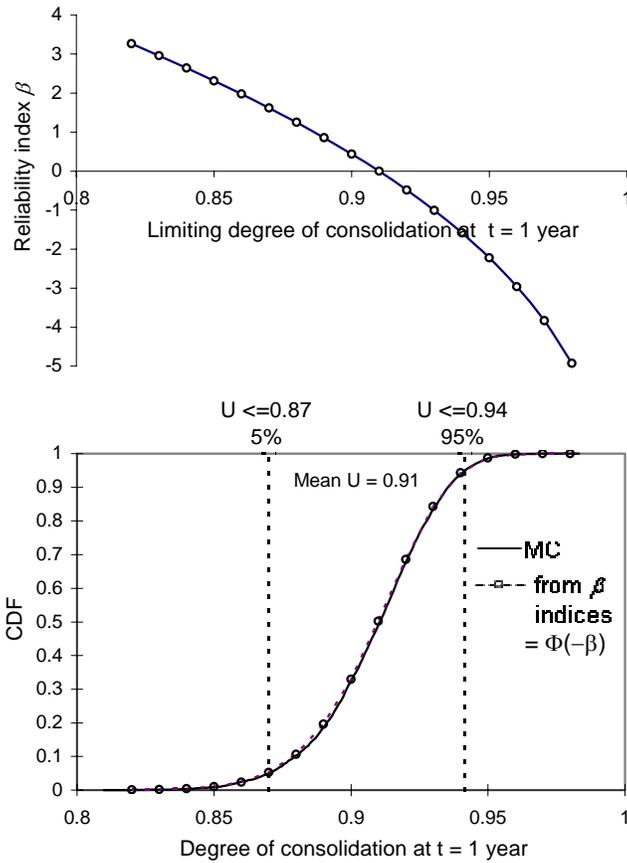
Fig. 11. Reliability indices for different limiting U at t = 1 year, and comparison of CDF based on β indices with CDF from Monte Carlo simulations.

Fig. 12. Reliability indices for different limiting settlement remaining at t = 1 year, and comparison of CDF based on β indices with CDF from Monte Carlo simulations.

It is of interest to note that the n_i values of c_v and c_h in cells AE30:AE31 of the lower Fig. 9 are practically zeros. The implied insensitivities of the ultimate consolidation settlement to c_v and c_h are theoretically consistent (ultimate settlement not a function of rate parameters c_v and c_h), and are automatically revealed in a reliability analysis. In contrast, reliability analysis with respect to limiting degree of consolidation at t = 1 year and settlement remaining at t = 1 year will show non-zero values for the n_i values of c_v and c_h, both parameters having an effect on the rate of consolidation.

Obtaining PDF Curves from β Index

The CDF curves shown in the lower plots of Figs. 10, 11 and 12 were obtained easily—by Eqs. (5), (6) and (7)—from the β values shown in the corresponding upper plots. In addition, it is simple to obtain the probability density function (PDF) of the respective outputs (s_{cf}, U and s_r), by applying cubic spline interpolation (e.g., Kreyszig 1988) to the CDF. This is accomplished easily in the Excel spreadsheet platform, as explained below with respect to the 19 CDF values of Fig. 10:

(i) Autofill a 17-cell column vector of m_i (i=2 to 18) with the following formula, next to the column of the 19 CDF values of s_{cf} :

$$m_i = \frac{3}{h}\left(CDF_{i+1} - CDF_{i-1}\right) \qquad (8)$$

in which h is the s_{cf} interval of the CDF points (= 0.2 m).

(ii) A 17×17 tridiagonal matrix $\underline{D}$ is set up, with entries $d_{i,i} = 4$, $d_{i+1, i} = d_{i, i+1} = 1$, and all other entries equal to 0.

(iii) The 17 PDF values are obtained immediately and automatically upon entering "=mmult(minverse($\underline{D}$),$\underline{m}$)" as a spreadsheet array formula in a 17-cell column.

The PDF curve of s_{cf} thus obtained is shown in Fig. 13. By the same procedure, 15 and 21 PDF values of the degree of consolidation (U) and of the settlement remaining (both at time = 1 year) were obtained easily from their respective 17 and 23 CDF values of Figs. 11 and 12. These two PDF curves are shown in Figs. 14 and 15.

The 5000 Monte Carlo realizations performed earlier for the plots of Figs. 11, 12 and 13 can also be used to plot the outputs as PDF curves. The dashed PDF curves derived from the β indices agree remarkably well with the Monte Carlo PDF curves in Figs. 13, 14 and 15.
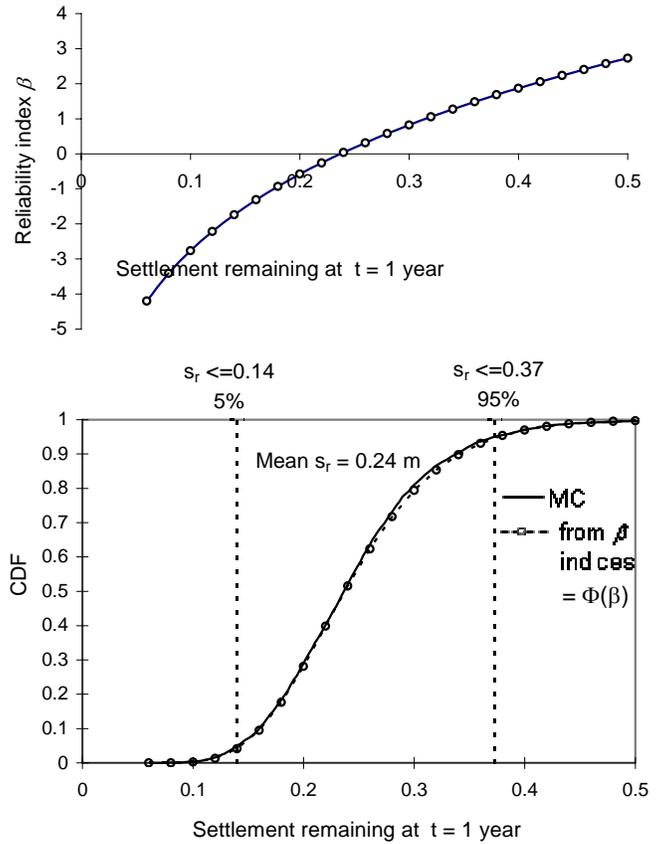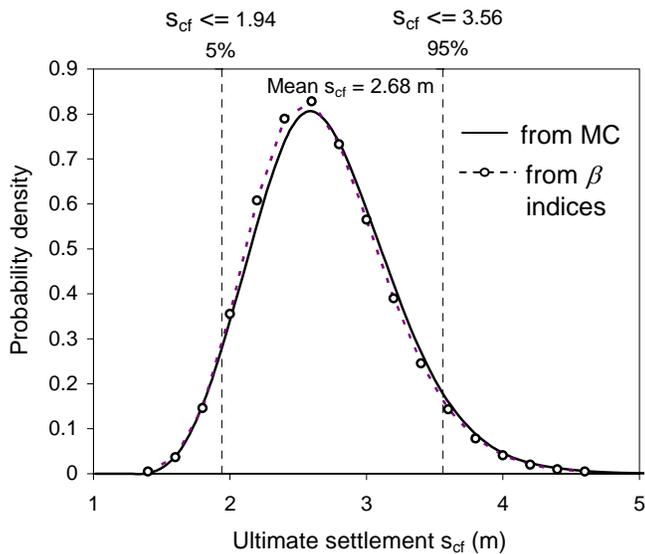
Fig. 13. PDF of ultimate primary consolidation settlement s_{cf}, from Monte Carlo simulations with 5000 realizations, and from 19 values of reliability index.
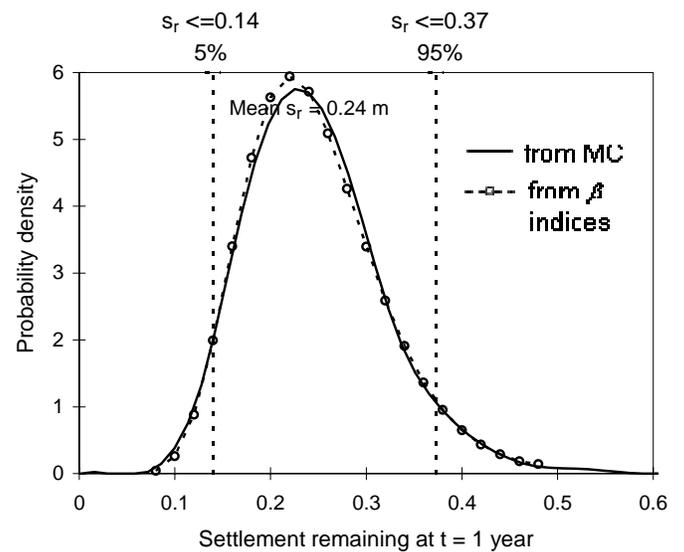

Fig. 15. PDF of settlement remaining (s_r) at time = 1 year, from Monte Carlo simulations, and from 23 values of reliability index.
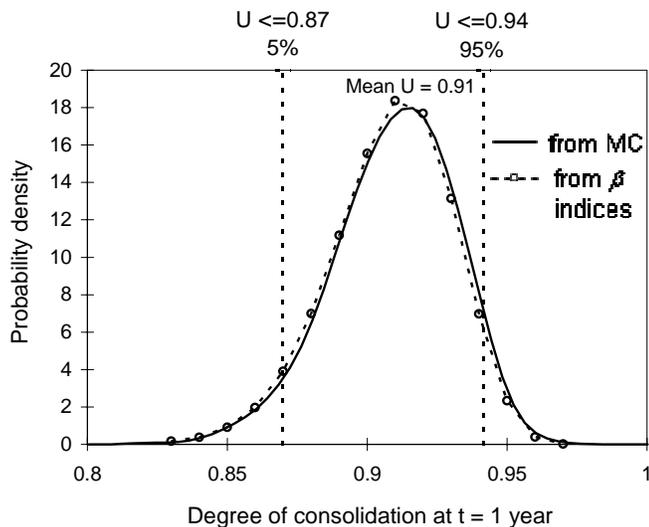

Fig. 14. PDF of degree of consolidation (U) at time = 1 year, from Monte Carlo simulations, and from 17 values of reliability index.

COUPLING OF STAND-ALONE DETERMINISTIC PROGRAM AND PROPOSED RELIABILITY METHOD VIA RESPONSE SURFACE METHOD

Programs can be written in spreadsheet to compute factor of safety or settlement (e.g., Low & Tang 2004 p.87, Low et al. 2007, and the *VDrainSt* program in this study). However, there are situations where serviceability or ultimate limit states can only be evaluated using stand-alone finite element or finite difference programs, or one may already have a preferred or more accurate deterministic program in hand. In these circumstances, reliability analysis and reliability-based design using the present approach can still be performed, provided one first obtains a response surface function (via the established response surface methodology) which closely approximates the outcome of the stand-alone finite element or finite difference programs. Once the closed-form response functions have been obtained, performing reliability-based design for a target reliability index is straightforward and fast. Performing Monte-Carlo simulation on the closed form approximate response surface function also takes little time. The response surface method was used by Li (2000) for consolidation analysis of a Singapore land reclamation project, Tandjiria et al. (2000) for laterally loaded single piles, and Xu and Low (2006) for embankments on soft ground.

SUMMARY AND CONCLUSIONS

A deterministic program written in the programming environment of the Excel spreadsheet software is able to capture the salient features (Figs. 3 and 4) of the measured rates of consolidation of the marine clay (installed with vertical drains) beneath the Chek Lap Kok test embankments. Other user-preferred deterministic programs can be used together with the probabilistic FORM procedure illustrated in this study.

In the deterministic analysis, the agreement between the computed and the instrumented results is better for the 1.5-m spacing vertical drain quadrant (Fig. 3) than for the 3-m spacing vertical drain quadrant (Fig. 4). The discrepancies can be further reduced if different compressibility parameters (C_R, C_{RR}) and rate parameters (c_v, c_h) are used. This was not done. Instead, first-order reliability analysis was performed to illustrate a new spreadsheet-based FORM algorithm (Low and Tang, 2007) as an efficient computational alternative to the classical mathematically-involved FORM procedure.

For the problem in hand, one can compute a reliability index β (and probability of unsatisfactory performance) with respect to a serviceability limit state (ultimate settlement magnitude or degree of consolidation). Alternatively, one can obtain the cumulative distribution (CDF) and probability density (PDF) of the magnitude and degree of consolidation settlement from a series of reliability index values (Figs. 10-12). It is important to distinguish negative from positive reliability index values. The computed reliability index should be treated as negative if the mean-value point is located in the unsafe domain.

The relationship between CDF and β index is either CDF = $\Phi(-\beta)$ or CDF = $\Phi(\beta)$, as discussed in connection with Eqs. (5)-(7). The relationship is exact for a plane limit sate surface and normally distributed random variables. Many geotechnical ultimate and serviceability limit state surfaces are nearly planar and good accuracy is often obtained when correlated nonnormals are dealt with via FORM.

The PDF is the derivative of the CDF. For a series of discrete CDF values, the PDF values can be solved conveniently using the simple three-step cubic-spline procedure explained in connection with Eq. (8). About 20 values of reliability index are sufficient to produce CDF and PDF curves (Figs. 10-15) which are as good as Monte Carlo simulation requiring thousands of realizations of outputs.

The spreadsheet-based reliability approach presented in this paper can operate on stand-alone numerical packages (e.g., finite element) via the response surface method, which is itself readily implementable in spreadsheet.

As in any analysis, the results of reliability analysis in this study depend on consolidation model and inputs (standard deviations, probability distribution types, and correlation matrix). Had different statistical inputs been used, the plots of β, CDF and PDF (Figs. 10-15) would be different. Nevertheless, even this qualified meaning of reliability index (and associated CDF and PDF) is more useful than a deterministic analysis which does not reflect uncertainties. The focus of this study is on illustrating a practical and intuitive FORM procedure in the context of a case history, and may contribute component blocks necessary for the final edifice of a comprehensive probabilistic approach. Other issues that deserve at least equal attention include model uncertainty and estimation of statistical inputs.

REFERENCES

Ang, H.S., and Tang, W.H. [1984]. *Probability Concepts in Engineering Planning and Design, Vol. 2-Decision, Risk, and Reliability*, Wiley, New York.

Baecher, G.B., and Christian, J.T. [2003]. *Reliability and Statistics in Geotechnical Engineering*. Wiley; Hoboken, N.J.

Choa, V., Wong, K.S., and Low, B.K. [1990]. New Airport at Chek Lap Kok, Geotechnical Review and Assessment, Consulting Report to Maunsell Pte Ltd., Singapore.

Der Kiureghian, A., Lin, H.Z., and Hwang, S.J. [1987]. "Second-Order Reliability Approximations", *J. Eng. Mech.*, ASCE, 113(8), 1208-1225.

Foott, R., Koutsoftas, D.C., and Handfelt, L.D. [1987]. "Test Fill at Chek Lap Kok, Hong Kong", *J. Geotech. Eng.*, ASCE, 113(2), 106-126.

GCO, April 1990. New Airport at Chek Lap Kok, Geotechnical Investigation, Preliminary Information, Volume II. Geotechnical Control Office, Civil Engineering Services Department, Hong Kong.

Haldar, A., and Mahadevan, S. [1999]. *Probability, Reliability and Statistical Methods in Engineering Design.* Wiley, N.Y.

Koutsoftas, D.C., Foott, R., and Handfelt, L.D. [1987]. "Geotechnical Investigations Offshore Hong Kong", *J. Geotech. Eng.,* ASCE, 113(2), 87-105.

Kreyszig, E. (1988). *Advanced Engineering Mathematics*, 6th ed., Wiley, 972-973.

Li, Guo-Jun [2000]. *Soft Clay Consolidation Under Reclamation Fill and Reliability Analysis*. Ph.D. thesis, School of CEE, Nanyang Technological University, Singapore.

Low, B.K. [2003]. Chapter 2: Theories, Computations, and Design Procedures Involving Vertical Drains. (In *Soil Improvement: Prefabricated Vertical Drain Techniques*, Bo, M.W., Chu, J., Low, B.K., and V.Choa, Thomson Learning.)

Low, B.K., and Tang, W.H. [2004]. "Reliability Analysis Using Object-Oriented Constrained Optimization", *Structural Safety*, Elsevier Science Ltd., 26(1), 69-89.

Low, B.K., and Tang, W.H. [2007]. "Efficient Spreadsheet Algorithm for First-Order Reliability Method", *J. Eng. Mech.*, ASCE, 133(12), 1378-1387.

Low, B.K., Lacasse, S., and Nadim, F. [2007]. "Slope reliability analysis accounting for spatial variation", *Georisk: Assessment and Management of Risk for Engineered Systems and Geohazards*, Taylor & Francis, London, 1(4), 177-189.

Rackwitz, R. [2001]. "Reliability Analysis—A Review and Some Perspectives", *Structural Safety*, 23, pp. 365-395, Elsevier Science Ltd.

Tandjiria V., Teh, C.I., and Low, B.K. [2000]. "Reliability Analysis of Laterally Loaded Piles Using Response Surface Methods." *Structural Safety,* Elsevier, 22(4), 335-355.

Xu, B. and Low, B.K. [2006]. "Probabilistic Stability Analyses of Embankments Based on Finite-Element Method", *J. Geotech. Geoenviron. Eng.*, ASCE, 132(11), 1444-1454.